Practical 3D Printing of Antennas and RF Electronics

Gregory Kiesel, Philip Bowden, Kevin Cook, Matt Habib, Jeramy Marsh, David Reid, Cameron Phillips, Brad Baker
Advanced Concepts Lab
Georgia Tech Research Institute
Atlanta, GA 30318
Gregory.Kiesel@gtri.gatech.edu

Abstract: *Recent advances in 3D printing technology now enable antennas and RF electronics to be designed and prototyped significantly faster than conventional manufacturing time scales. New printers and materials on the market now provide affordable access to RF rapid prototyping. In this paper, tools and techniques are shown which simplify the design process for 3D printed antennas, and RF devices. Three example RF components are fabricated and evaluated: a Marchand balun, a monopole array antenna and a Ku-band bow tie antenna.*

Keywords: 3D Printing; Rapid Prototyping; Antennas; Arrays; Passive RF; Combiners

Introduction

Additive manufacturing can reduce the time and material costs in a design cycle and enable the on-demand printing of customized parts. New multi-material 3D printers that can print both metal and dielectric materials enable the additive manufacturing of antennas [1] and RF components [2]. Developments in software are critical to leveraging this capability; good tools allow more effort to go towards creation than implementation.

Three devices are described in detail in this paper to demonstrate the 3D printing of RF components. A Marchand balun [3] is presented demonstrating rapid prototyping of a complex multi-layer RF circuit. A monopole array is shown with an integrated beam steering network [4] and radome to show rapid prototyping of a complete antenna system. A bow tie antenna with rounded corners [5] is presented showing good performance in the Ku-band.

The devices in this paper were made with a Voxel8 [6] printer and materials. In the final section, the Voxel8 printer's tolerances and electrical properties are presented.

Design Process

Several existing tools and sites provide the ability to customize mechanical structures; this concept is expanded into the RF domain with software that uses a high-level design parameter to create the circuit, model the performance, and create Computer Assisted Manufacturing (CAM) files. By intelligently leveraging this process, the design can be readily updated or customized after the initial development. A Computer Assisted Drafting (CAD) tool may further modify the structure to customize the mechanical interface and a machine toolpathing code (a slicer) is used to translate the CAM files to a format the printer can use. The monopole array with an integrated beam forming network and radome is specifically used to illustrate the process that is used for each component presented.

Design Tool: A custom frequency-domain circuit simulation code has been developed which uses a schematic input (Figure 1) to model a circuit's S-Parameters. The design tool handles variables, calculations, and can perform optimizations; the modeled results for the monopole array are plotted (Figure 2). The tool can automatically generate the layout from the schematic and can create Stereo-lithography (STL) files for both the metal and the plastic materials. The overall design process is simplified significantly since the same schematic / tool is both modeling the device and creating all of the CAM files without requiring a CAD specific tool such as SolidWorks.

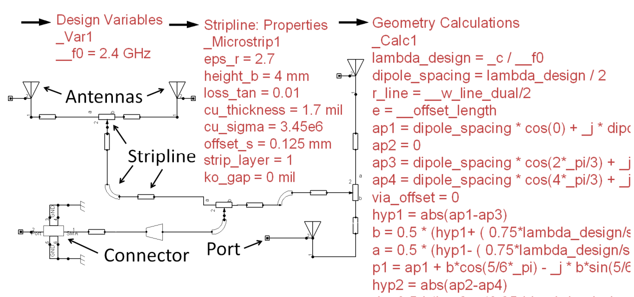

Figure 1: Simulation and artwork generation tool

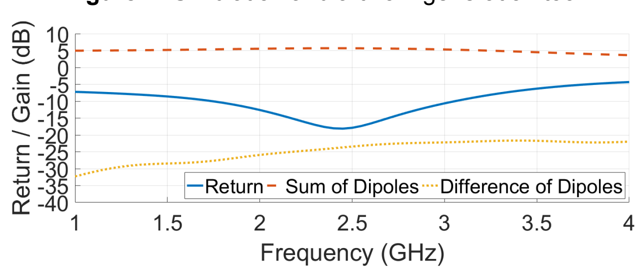

Figure 2: Modeled gain and input match for the monopole array.

The monopole array schematic shown in Figure 1 has three sets of variables: design, material and geometry. The design variables are the inputs most likely to be modified, such as the center frequency of operation. The material variables are an example of inputs that change infrequently,

Distribution A: Approved for public release; distribution unlimited.

for example if the design process shifted to a different plastic. Finally, a series of calculations are needed that define the geometry and altering these fundamentally defines a different product; these calculate the dipole positions, line widths and line lengths (Figure 3).

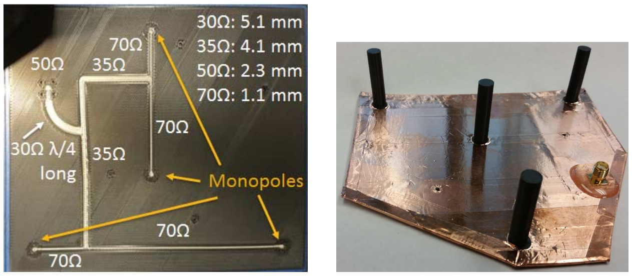

(a) (b)

Figure 3: Stripline layer captured mid-print (a) and final array with copper tape ground on top and bottom (b).

CAD Tool: If needed, the mechanical design can be further modified. The schematic above creates the traces, monopoles and radome but not mounting holes. Figure 4 shows a view of OpenSCAD, a free CAD tool that uses code to describe mechanical structures. In this example, the location of the mounting holes is easily modified through a few straightforward variables. This simplifies the process of integrating the design to a new platform. While this process simplifies minor changes in form factor, care must be taken not to break the RF performance.

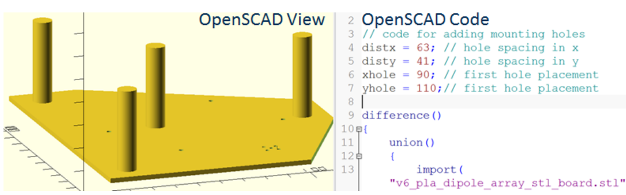

Figure 4: OpenSCAD is used to add the mounting holes

Slicing Tool: The final software tool needed is a machine toolpathing algorithm (slicer) to translate the mechanical CAM files into the machine control language of the 3D printer. These prints used Euclid, which is the slicer provided by Voxel8. Euclid dynamically modulates the plastic layer heights to ensure the accurate spatial positioning of the silver ink, which is important for the Marchand balun (below). Euclid automatically performs subtractive Boolean operations that create cavities in the plastic to ensure proper clearances for printed silver features, electrical components, and printhead geometries. Performing the Boolean operations in the slicer simplifies the requirements of STL generation for the design tools which enables the use of many different 3D design processes.

Components and Systems

Three example components are presented in this section to validate the performance of the tools and hardware: an L-band balun, an S-band antenna array and a Ku-band antenna element.

Marchand Balun: A Marchand balun is a reasonably broadband device made out of coupled lines and used in many RF applications. This design used broadside coupled striplines (Figure 5) which intrinsically isolate the lines from stray coupling. The printed structure was wrapped in copper tape (Figure 3b) to provide the upper and lower ground planes. Three through-hole connectors were attached using conductive ink and epoxy. The design had good performance as a balun over the design band of 1.5 GHz – 2 GHz (Figure 6 and Figure 7).

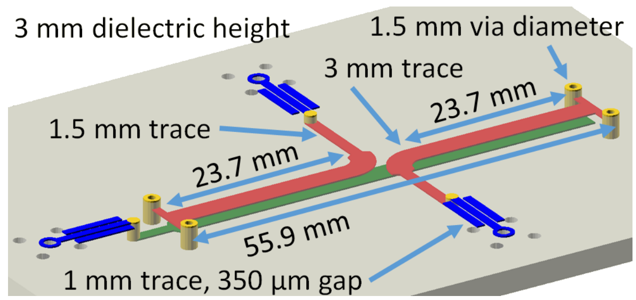

Figure 5: CAD view of a stripline Marchand balun with two stripline inner layers (green and red) and a top layer coplanar waveguide section (blue).

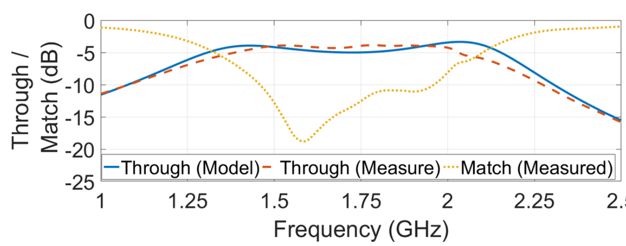

Figure 6: Measured gain and match for the Marchand balun.

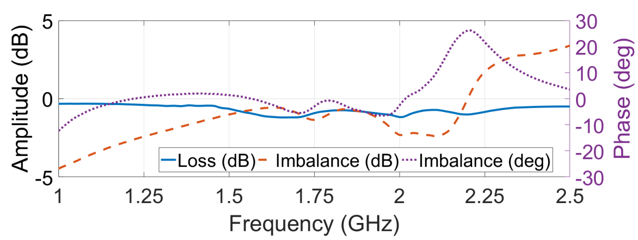

Figure 7: Measured loss, amplitude balance, and phase balance for the Marchand balun.

Monopole Array with Integrated Beam Former: A lightweight WiFi directional array was constructed with mounting holes for a 3DR Solo UAV. Monopoles were used to keep wind loading low. The device was constructed to be directional and to provide a null (Figure 8) which can be useful for improving the link, direction finding, or interference suppression. The location of the four quarter-wave monopoles is calculated based on the design frequency, and the line lengths of the combiner provide a true time delay sum in the desired direction. The device had a good match (Figure 9) and pattern (Figure 10).

The monopoles for this array are 31 mm tall. The three outer monopoles are a half-wavelength from the center element and 120° in angle from each other. The dimensions for the trace widths are shown in Figure 3a. The dielectric height for the stripline section was 4 mm.

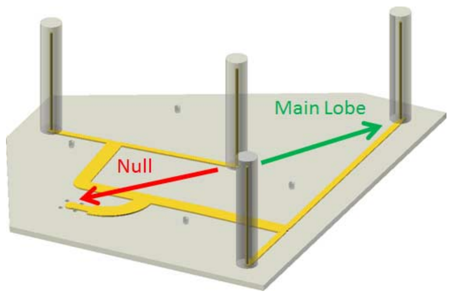

Figure 8: CAD view of a four-monopole array with an integrated stripline beamforming network.

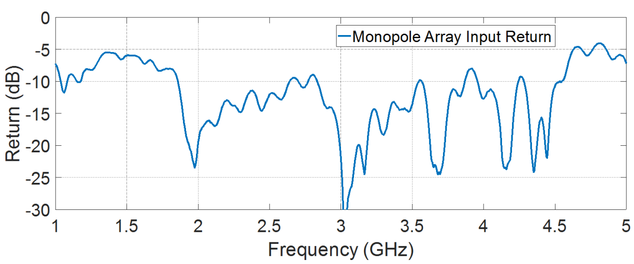

Figure 9: Measured Return Loss for the monopole array

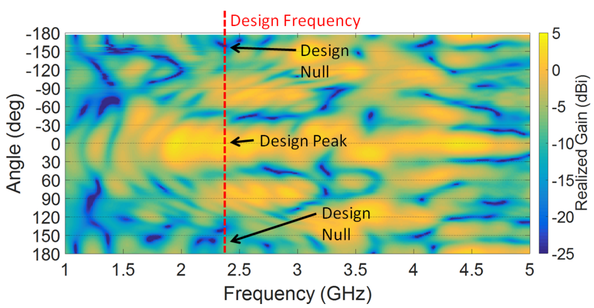

Figure 10: Measured gain pattern over frequency and angle.

Ku-band bowtie: A bow tie antenna was constructed to characterize the printer's ability to make higher frequency antennas (Figure 11). The antenna was modeled with Ansys HFSS and good agreement was found through Ku-band. The dimensions are shown in Figure 12.

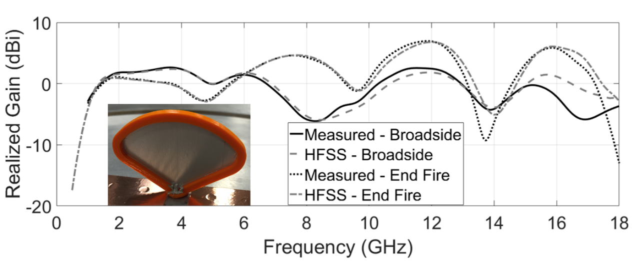

Figure 11: Measured and modeled gain of a printed bow tie antenna.

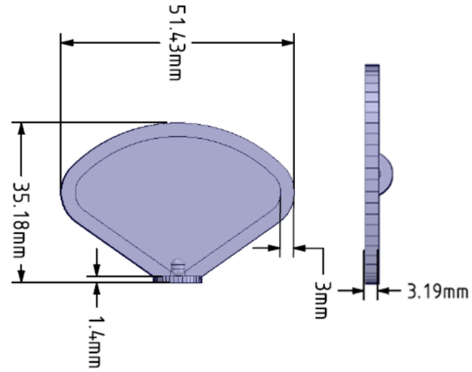

Figure 12: Dimensions of the printed bow tie antenna.

Capabilities of the Voxel8 Printer

While the concepts described in this paper are by no means restricted to a single process, it is worthwhile to examine the specific process used to validate our designs.

Electrical Properties: The permittivity and conductivity of the materials used were measured in a variety of ways and all showed agreement. All measurements have been taken with printed material (as opposed to raw stock).

The plastic used for these prints is Polylactic acid (PLA), which is popular for prototyping in part because it has less toxic fumes than other plastics [7]. The initial measurement used a focused beam system (Figure 13) to measure the permittivity for four colors of PLA, each approximately 3.1 mm thick. These values were validated with a coaxial airline technique and through the measure-model agreement of the various RF circuits.

Voxel8 Standard Silver Ink was used for these prints, a room temperature curing silver conductive ink. The vendor lists the DC conductivity as 3.45 MS/m. A 250 µm thick board with a 1.5 mm wide, 71 mm long microstrip line constructed and measured to back out the conductivity of the silver ink, and Figure 14 shows good agreement using 3.45 MS/m in a simulation that agrees with the measurement. For reference, pure silver has a conductivity of 61 MS/m.

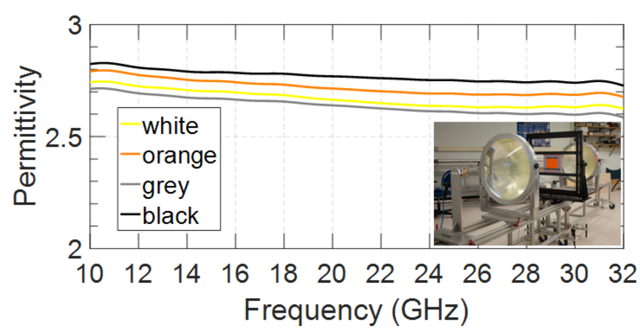

Figure 13: Permittivity of different color PLA samples. Inset shows a focused beam system used to measure the samples.

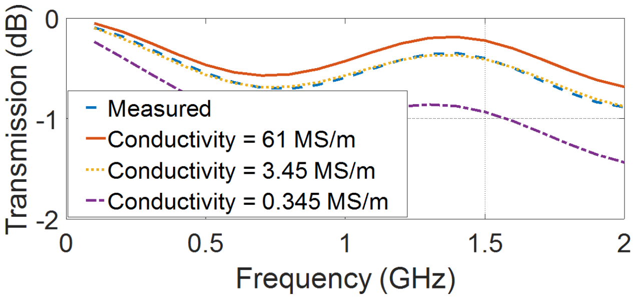

Figure 14: Measured Voxel8 microstrip line compared against finite element models using 61 MS/m (pure silver), 3.45 MS/m and 0.345 MS/m

Mechanical Tolerances: When designing printed circuit boards, it is common to consider the trace and space tolerances, that is, the accuracy to which one can maintain a desired trace width and the gap between traces. Because the 3D printer deposits the ink with a 0.25 mm nozzle, it should be expected that small traces might not print as designed. The vendor recommends 0.5 mm lines for general prints (two passes); however, RF circuits generally require more design flexibility.

Three test boards were printed to measure the trace and space tolerances and were characterized with a Keyence digital optical microscope used as a profilometer. The measured trace width tolerances are shown in Figure 15 and the spacing tolerances are shown in Figure 16. The gap measurements were averaged along the lines; at 100 µm the lines were sporadically shorted. Below 1 mm line widths had poor accuracy although from Figure 17 we see from an RF standpoint it's acceptable above 800 µm. Gaps at 100 µm were not reliable but accuracy was good above 100 µm.

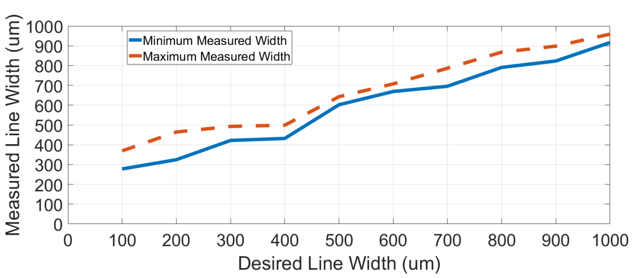

Figure 15: Measured line width versus desired line width

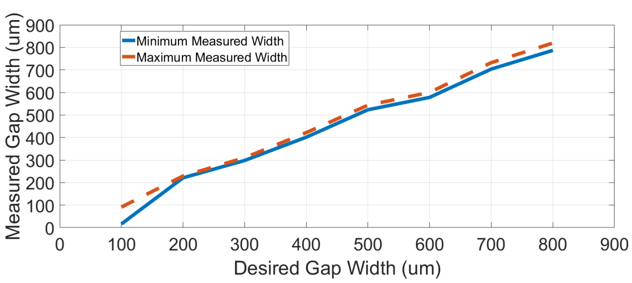

Figure 16: Measured spacing versus desired gaps

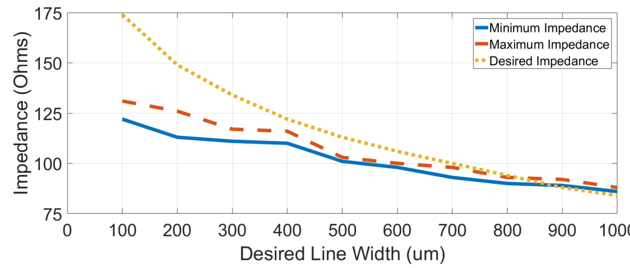

Figure 17: Realized impedance versus design impedance for microstrip lines on PLA.

Conclusion

Useful RF and antenna structures can be 3D printed which has the potential to revolutionize the design, supply and sustainment phases of an acquisition program. A design process was presented which demonstrates how this technology can be utilized to support customization in the field. A Voxel8 printer was used to construct a balun demonstrating a complex 3D printed structure, a monopole array demonstrating a complete antenna system and a bowtie antenna demonstrating Ku-band performance.

References

1. Nassar, I.T.; Weller, T.M., "An electrically-small, 3-D cube antenna fabricated with additive manufacturing," Radio and Wireless Symposium, no., pp.262,264, 20-23 Jan. 2013.
2. N. Arnal, T. Ketterl, Y. Vega, J. Stratton, C. Perkowski, P. Deffenbaugh, et al., "3D multi-layer additive manufacturing of a 2.45 GHz RF front end," in Microwave Symposium (IMS), 2015 IEEE MTT-S International, 2015, pp. 1-4.
3. N. Marchand, "Transmission line conversion transformers," Electronics, vol. 17, no. 12, pp. 142–146, Dec. 1944.
4. D. M. Pozar, Microwave Engineering, 2nd ed. New York: Wiley, 1998.
5. S. W. Qu and C. L. Ruan, ―Effect of Round Corners on Bowtie Antennas, Progress In Electromagnetics Research, PIER 57, Pp. 179–195, 2006.
6. Voxel8 makes 3D printing hardware, software and materials. http://www.voxel8.com/
7. Brent Stephens, Parham Azimi, Zeineb El Orch, Tiffanie Ramos, "Ultrafine particle emissions from desktop 3D printers," Atmospheric Environment, vol. 79, November 2013, pp. 334-339.